Published in final edited form as:
Peptides. 2011 September ; 32(9): 1840–1848. doi:10.1016/j.peptides.2011.08.010.

An Integrin-binding N-terminal Peptide Region of TIMP-2 Retains Potent Angio-Inhibitory and Anti-tumorigenic Activity *In Vivo*

Dong-Wan Seo, Ph.D., **W. Carl Saxinger, Ph.D.**[b], **Liliana Guedez, Ph.D.**, **Anna Rita Cantelmo, Ph.D.**[c], **Adriana Albini, Ph.D.**[c], and **William G. Stetler-Stevenson, MD, Ph.D.**[a,*]

[a]Radiation Oncology Branch, Advanced Technology Center, CCR, NCI, NIH, Bethesda, MD 20892, USA

[b]Basic Research Laboratory, Frederick Cancer Research Facility, Bldg. 1052, Frederick, MD 21702

[c]Resp Ricerca Oncologica, IRCCS Multimedica, Milan, Italy

Abstract

Tissue inhibitor of metalloproteinases-2 (TIMP-2) inhibits angiogenesis by several mechanisms involving either MMP inhibition or direct endothelial cell binding. The primary aim of this study was to identify the TIMP-2 region involved in binding to the previously identified receptor integrin α3β1, and to determine whether synthetic peptides derived from this region retained angio-inhibitory and tumor suppressor activity. We demonstrated that the N-terminal domain of TIMP-2 (N-TIMP-2) binds to α3β1 and inhibits vascular endothelial growth factor-stimulated endothelial cell growth *in vitro*, suggesting that both the α3β1-binding domain and growth suppressor activity of TIMP-2 localize to the N-terminal domain. Using a peptide array approach we identify a 24 amino acid region of TIMP-2 primary sequence, consisting of residues Ile43-Ala66, which shows α3β1-binding activity. Subsequently we demonstrate that synthetic peptides from this region compete for TIMP-2 binding to α3β1 and suppress endothelial growth *in vitro*. We define a minimal peptide sequence (peptide 8–9) that posses both angio-inhibitory and, using a murine xenograft model of Kaposi's sarcoma, anti-tumorigenic activity *in vivo*. Thus, both the α3β1-binding and angio-inhibitory activities co-localize to a solvent exposed, flexible region in the TIMP-2 primary sequence that is unique in amino acid sequence compared with other members of the TIMP family. Furthermore, comparison of the TIMP-2 and TIMP-1 protein 3-D structures in this region also identified unique structural differences. Our findings demonstrate that the integrin binding, tumor growth suppressor and *in vivo* angio-inhibitory activities of TIMP-2 are intimately associated within a unique sequence/structural loop (B-C loop).

[*]To whom correspondence should be addressed: Radiation Oncology Branch, Center for Cancer, Research, National Cancer Institute, Advanced Technology Center, 8717 Grovemont Circle, Bethesda, MD 20892-4605; Voice: 301-402-1521; Fax: 301-435-8036; sstevenw@mail.nih.gov.
[1]Present Address: Department of Molecular Bioscience, Institute of Bioscience and Biotechnology, College of Biomedical Science, Kangwon National University, Chuncheon 200-701, Republic of Korea

Conflict of Interest
The authors declare that there are not competing financial interests in relation to the work described.

Supporting Information Available:
Supplemental Table 1: Peptide Array Sequences
Supplemental Table 2: Additional Peptide Sequences

Keywords

Angiogenesis; Angiogenesis Inhibitors; Tissue Inhibitor of Metalloproteinases-2 (TIMP-2); peptide inhibitors; Kaposi's Sarcoma

1. Introduction

The tissue inhibitors of metalloproteinases (TIMPs) are a small family of four proteins that are well characterized as inhibitors of the matrix metalloproteinase (MMP) family, and some members of a disintegrin and metalloproteinase (ADAMs) family [2, 20]. The MMP inhibitory activity accounts for the ability of TIMPs to inhibit angiogenesis and tumor progression. However, recent studies have shown that TIMPs also directly regulate cell behavior, independent of their proteinase inhibitory activity [2, 20, 30]. TIMP-2 is a unique member of the TIMP family in that it directly inhibits endothelial cell proliferation *in vitro* and angiogenesis *in vivo* [30].

Previous studies demonstrate that TIMP-2 suppresses the proliferation of endothelial cells, fibroblasts, and carcinoma cell lines in response to stimulation with mitogenic growth factors *in vitro* [15, 28, 34]. TIMP-2 binds to the surface of human microvascular endothelial cells (hMVECs) via interaction with the integrin α3β1 and this interaction mediates suppression of FGF-2- or VEGF-A-induced hMVEC proliferation *in vitro* and angiogenesis *in vivo* [28]. This angio-inhibitory effect is entirely independent of TIMP-2-mediated inhibition of MMP activity as the use of the Ala+TIMP-2 mutant, which lacks MMP inhibitory function, retains equally effective angio-inhibitory activity *in vitro* and *in vivo* [28, 34]. This effect involves a second TIMP-2-mediated mechanism known as integrin-mediated heterologous receptor inactivation. Specifically, TIMP-2-binding to integrin α3β1 mediates inactivation of receptor tyrosine kinases (FGFR-1 or VEGFR-2). Receptor inactivation occurs through dephosphorylation of tyrosine residues by protein tyrosine phosphatase (PTP) activity, identified as the SH-2 domain phosphatase known as Shp-1 [28, 29].

The structure of TIMP-2, like other members of the TIMP family consists of six disulfide loops which are divided into an N-terminal domain, consisting of the first three disulfide loops that retains MMP inhibitory activity, and a C-terminal domain, that also consists of three disulfide loops, which can mediate binding to the hemopexin-like domains of several members of the MMP family [2, 5, 6, 20]. The N-terminal domain of all TIMP family members is an oligonucleotide/oligosaccharide-binding (OB) fold structure in which the N-terminal domain is dominated by a β-barrel structure and the mechanism of MMP inhibition involves co-ordination of the zinc atom at the active site by the amino group of the N-terminal cysteine residue [2, 10, 12, 31]. MMP inhibitory activity is dependent upon the correct three-dimensional structure and a free amino terminal cysteine. Work by Fernandez and colleagues demonstrates that the angio-inhibitory effect of TIMP-2 is dissociable from MMP inhibition [8], and these authors localize TIMP-2 angio-inhibitory activity to the C-terminal cysteine loop (loop 6) of the protein structure. Recently, the mechanism of this anti-angiogenic activity was shown to involve binding of 24-mer peptide of loop 6 to the insulin-like growth factor-1 receptor (ILGF-1R) [9]. Therefore, we undertook the present study to identify the region of the TIMP-2 protein involved in integrin binding and determine if this integrin-binding region, like loop 6 peptide, retained endothelial growth suppressive activity and angio-inhibitory activity *in vivo*.

2. Materials and Methods

2.1 Cell lines and growth factors

Human microvascular endothelial cells (hMVECs) and growth factors were purchased from commercial sources and used as previously described [28]. TIMP-2, as well as Ala+TIMP-2, were prepared and characterized as described previously [34]. The N-terminal domain of TIMP-2 (Cys^{1}–Cys^{126}) referred to as N-TIMP-2 and C-terminal TIMP-2 domain (Glu^{127}-Pro^{194}), referred to as C-TIMP-2, fused to C-terminus of glutathione-s-transferase were prepared using similar expression and purification techniques as were used for the full length proteins [34], with final reverse phase chromatography purification. The TIMP-2 and N-TIMP-2 preparation retained MMP inhibitory activity as previously reported [6, 34].

Integrin α3β1 (Chemicon) was diluted in 25 mM Tris HCl, 150 mM NaCl, 0.1 mM $CaCl_2$, 1 mM $MgCl_2$, 10 mM octyl-β-d-glucopyranoside and labeled with $Na^{125}I$ using IODO Beads iodination reagent (Pierce, Rockford, IL) according to the manufacturer's instructions.

2.2 Protein binding and peptide array integrin-binding assays

To examine the direct binding of ^{125}I-α3β1 to TIMP-2 proteins and in peptide competition experiments, these protein binding assays were performed as previously described using Ca^{+2} and Mg^{+2} containing PBS [28]. The individual wells were then incubated with 2 nM ^{125}I-α3β1 for 2 h at 37°C. Plates were then washed 3X with binding buffer, and the remaining bound ^{125}I-α3β1 was quantified by γ counting. The peptide array plates were then assayed for ^{125}I-α3β1 exactly as described for the protein binding assay, with the exception that the incubation was for 30 min at 37°C, and the bound ^{125}I-α3β1 was extracted from each well by incubating with 100 μL 10% SDS, 2 M Urea and 0.5% 2-mercaptoethanol, before being quantified by γ counting. All data were corrected for non-specific background binding and specific activities of ^{125}I-α3β1 preparations. Failure to include divalent cations in the binding buffer significantly reduced binding of both proteins and peptides. Failure to include divalent cations in the binding buffer significantly reduced binding of both proteins and peptides, consistent with the conclusion that binding is divalent cation-dependent.

2.3 Cell growth assays

The hMVECs growth assays were performed using Cell-Titer 96 Aqueous One Solution reagent (Promega) exactly as previously described [28]. The results from six replicate determinations of cell number (mean ± standard deviation) are presented as the fold-increase of non-stimulated growth, or as the percentage of maximal growth factor-stimulated growth if comparison between separate experiments was necessary.

2.4 Peptide array synthesis

Peptide arrays composed of 18-mer peptides with twelve amino acid residue overlaps were synthesized in 96-well plate format using previously characterized methodology [19, 26, 27]. In this method the peptides are linked to the surface of the 96-well plate via a polylysine linker, to prevent steric restriction of access to the TIMP-2 peptide sequence. The average molecular tether consists of 50 lysine residues. The peptides of interest are then synthesized using FMOC methodology and the average yield is approximately 380 pmoles/well [27]. The sequences of the peptides in each well of the plates for the TIMP-1 and TIMP-2 peptides are listed in Supplemental Table 1.

2.5 Synthetic peptide synthesis

All synthetic peptides (Supplemental Table 2) were obtained from a commercial laboratory (Peptide Technologies Corporation, Gaithersburg, MD). The peptides were purified to >97%

homogeneity by reverse phase chromatography and the sequences confirmed by mass spectroscopy analysis.

2.6 Directed in vivo angiogenesis assays

In vivo angiogenesis assays were performed using the directed *in vivo* angiogenesis assay (DIVA assay) in athymic nude (*nu/nu*) mice and using VEGF-A (500 ng/mL) as an angiogenic stimulus as previously described [14]. Experiments were normalized against maximal angiogenic response to VEGF-A (positive control) to allow direct comparison between independent experiments.

2.7 Amino acid sequence and protein structure analysis

TIMP protein sequences were analyzed using the ClustalW alignment program (Gonnet Similarity Matrix) in MacVector™ (v9.5.2 with default settings).

Structure coordinates for TIMP-2 (file 1BR9) and TIMP-1 (file 2JOT) were downloaded from the Collaboratory for Structural Bioinformatics Protein Data Base home page (URL: http://www.rcsb.org/pdb/home/home.do) and aligned using the Swiss Protein Data Base Viewer (http://ca.expasy.org/spdbv/text/download.htm). Images were saved as PICT files and labeled using Microsoft PowerPoint™ software.

2.8 Kaposi's sarcoma model of tumor growth

The anti-tumorigenic activity of Peptide 8–9 was assayed using the highly angiogenic Kaposi's sarcoma described previously [11]. Treated animals were given 150 μL of 500 nM Peptide 8–9 dissolved in vehicle (PBS containing 0.1% polyethylene glycol) 3 times a week starting at day 0. Controls received the same volume of vehicle and each group contained eight animals. Tumor growth was monitored at regular intervals using calipers and tumor volumes were calculated using a rational ellipse formula (Tumor volume = (width^2 × length) × 0.5). On day 15 the animals were sacrificed and the tumors removed, weighed, and processed for histological examination.

2.9 Statistical analysis

All statistical analyses were performed using Prism™ 4.0 statistical software package (GraphPad, Inc.).

3. Results

3.1 N-terminal domain of TIMP-2 retains integrin-binding activity

We compared the ability of Ala+TIMP-2 (or TIMP-2, data not shown), N-TIMP-2 and C-TIMP-2 to bind ^{125}I-labeled α3β1 integrin using Maxisorb™ 96-well plates. The coating concentration of N-TIMP-2 was 0.4 μM compared with 1 μM for both Ala+TIMP-2 and C-TIMP-2, Figure 1a. ^{125}I-labeled α3β1-binding was two fold higher in the N-TIMP-2 coated wells compared with the Ala+TIMP-2 and three fold higher compared with C-TIMP-2. Statistical analysis (student t test) demonstrates that these differences are highly significant ($p<0.0001$).

To determine the efficiency of coating and estimate the binding affinity we performed a dose-response experiment using different coating concentrations of N-TIMP-2. Figure 1b demonstrates that integrin α3β1 binding to the N-TIMP-2 occurred in a linear and concentration-dependent manner ($R^2 = 0.988$). Using the specific activity of the ^{125}I-α3β1 preparation and assuming saturation binding of the N-TIMP-2 to the Maxisorb™ plates, we calculated the dissociation constant for each of the binding concentrations tested, Figure 1b

legend. The mean calculated K_D ~ 0.220 ± 0.118 nM for these experiments was in excellent agreement with previously observed dissociation constants for TIMP-2 binding to the cell surface [7, 15, 28]. If we reduced the estimated binding of the N-TIMP-2 to 50%, the K_D values remained in the low nanomolar range (K_D = 1.9–9.7 nM). These findings suggested that an α3β1 integrin-binding domain of the TIMP-2 molecule is located within the N-terminal domain and that the binding of N-TIMP-2 protein to the wells of the Maxisorb™ plates was at least moderately efficient (>50%) and more likely highly efficient (>90%). Furthermore, removal of the C-terminal domain enhanced the α3β1-binding activity.

3.2 N-terminal domain of TIMP-2 retains anti-mitogenic activity in VEGF-A-stimulated human microvascular endothelial cells

The data presented in Figures 1a and 1b suggested that the α3β1 integrin-binding domain of the TIMP-2 protein was located within the first 126 amino acid residues comprising the N-terminal domain. To determine if N-TIMP-2 also has growth inhibitory activity we tested the ability of N-TIMP-2 to inhibit VEGF-A-stimulated mitogenesis of hMVECs *in vitro*, Figure 1c. Comparison of the ability of Ala+TIMP-2 and N-TIMP-2 to inhibit cell growth demonstrated that 100 nM final concentration of both proteins results in 75 and 67% inhibition of the two-fold increase in cell number observed following treatment with 10 ng/mL VEGF-A. Student t-test analysis again demonstrated that these effects were highly significant ($p<0.0001$), but that the difference between inhibition by Ala+TIMP-2 and N-TIMP-2 was not significant ($p= 0.473$). This finding suggests that the N-terminal domain retains potent growth suppressive activity that is essentially equipotent to Ala+TIMP-2 *in vitro*.

3.3 Peptide array analysis identifies TIMP-2 peptides that bind integrin α3β1

Previous studies show that the TIMP-2 growth suppression and integrin binding activities require expression of the α3 and β1 integrin subunits and can be competed by α3β1 blocking antibodies [28, 29], the question remains if the integrin-binding and growth suppressive activities involve similar regions of the TIMP-2 molecule. To address this issue we began with identification of the TIMP-2 integrin-binding region by utilizing a peptide array approach. Peptide arrays composed of 18-mer peptides with twelve amino acid residue overlaps were synthesized in 96-well plate format using previously characterized methodology [19, 26, 27]. Separate 96-well plate arrays for entire 194 amino acids of the mature TIMP-2 coding sequence and 184 amino acids of TIMP-1 were synthesized and probed for integrin binding-activity utilizing ^{125}I-α3β1. The corrected binding data were used to generate a ^{125}I-α3β1 integrin-binding profile. The profile for the TIMP-2 peptide array showed a definite peak in ^{125}I-α3β1 integrin-binding for the peptide sequence A-9 (designated as peptide 9) with substantial integrin binding on the adjacent N-terminal wells A-8 and A-7 (designated as peptides 8 and 7, respectively), Figure 2. Peptide 7 was not studied further as the 12 amino acid overlap that it is has in common with peptide 8 is not present in peptide 6 which showed markedly reduced integrin-binding activity. A dramatic decrease in integrin binding in wells corresponding to peptide sequences immediately C-terminal of peptide 9 (wells A-10, A-11, etc.) was also observed. The significance of this was further explored using additional synthetic peptides (vide infra).

In the TIMP-1 profile several isolated peaks of ^{125}I-α3β1 integrin-binding were observed, however, ^{125}I-α3β1-binding in adjacent wells containing peptide sequences that share 66% sequence identity was very low or absent, suggesting that the binding observed in these wells was a non-specific effect. Furthermore, TIMP-1 did not demonstrate suppression of hMVEC proliferation *in vitro*.

3.4 Competitive synthetic peptide binding assays confirm the α3β1-binding activity of TIMP-2 peptides

In order to confirm the ability of various peptides to bind to the ^{125}I-α3β1 integrin we utilized Ala+TIMP-2-coated 96-well plates in a binding competition assay. As seen in Figure 3, peptides 8, and the region of overlap between peptides 8 and 9 (designated peptide 8–9) at 1 μM concentration strongly compete for binding of the ^{125}I-α3β1 integrin, with >97% inhibition ($p<0.0005$). This level of inhibition is similar to that observed with 100 nM N-TIMP-2 previously demonstrated to have potent α3β1 integrin-binding activity, Figure 1a and 1b. Peptide 9 also demonstrates significant competition for α3β1 integrin-binding (~75%, $p<0.0005$).

Since the peptides immediately C-terminal of peptide 9 showed a dramatic decrease in direct α3β1 integrin-binding we attempted to confirm this apparent boundary for the TIMP-2 integrin-binding domain. To this end, we used three synthetic peptides: 1) The first designated peptide 9–13 contains the eight C-terminal residues of peptide 9 plus the next 15 residues of the TIMP-2 sequence; 2) Next we used a scrambled version of this peptide, designated peptide 9–13 SCR, in which the amino acid sequences of peptide 9–13 were randomly rearranged; 3) Finally, we made a peptide consisting of the final nine C-terminal amino acid residues of peptide 9–13, which are contained within peptides 11, 12 and 13 in the original array and hence designated peptide 11–13 (see Supplemental Table 2). The competition binding experiments show that peptide 9–13 retained statistically significant ($p<0.005$) competitive activity, Figure 3. However, if the sequence was scrambled or the peptide 9 sequence was removed from the peptide, these peptides (peptide 9–13 SCR and peptide 11–13, respectively) loose the ability to compete for binding of α3β1 integrin, Figure 3. These findings confirm the C-terminal boundary of the α3β1 integrin-binding domain that was first observed in the peptide array data.

3.5 TIMP-2 integrin-binding peptides retain anti-mitogenic activity in VEGF-A-stimulated human microvascular endothelial cells

We now tested the ability of the TIMP-2 peptide identified in the α3β1-peptide binding arrays to retain anti-mitogenic activity following VEGF-A stimulation of hMVECs and anti-angiogenic activity *in vivo*. Figure 4a demonstrates peptides 8, 8–9 and 9 at 1 μM concentration inhibited VEGF-A-stimulated mitogenesis in a statistically significant (>50% inhibition, $p\leq0.01$) manner, and were essentially equipotent as Ala+TIMP-2 (100 nM, ANOVA analysis $p= 0.2734$). We have previously shown that TIMP-2 and Ala+TIMP-2 also suppressed FGF-2-stimulated mitogenesis of hMVECs [28]. Peptides 8, 8–9 and 9 show similar growth suppressive activity against this mitogen as demonstrated for VEGF-A (data not shown). As we previously demonstrated for the integrin binding activity, the boundary sequence, peptide 9–13, containing the peptide 9 sequence (C-terminal eight amino acid residues) retained significant growth inhibitory activity (>95%, $p<0.005$), Figure 4b. However, if the sequence is scrambled (peptide 9–13 SCR) or peptide 9 sequence is deleted (peptide 11–13) the ability of these peptides to inhibit FGF-2-stimulated cell growth is greatly compromised ($p>0.17$). These data are compiled from two independent experiments and therefore the results were normalized to maximal growth response in each experiment for comparative purposes and are expressed relative to maximal growth activity of FGF-2 stimulation.

3.6 TIMP-2 integrin-binding peptides retain anti-angiogenic activity *in vivo*

Finally, we tested the ability of these TIMP-2 α3β1 integrin-binding peptides to inhibit angiogenesis *in vivo* utilizing the quantitative, directed *in vivo* angiogenesis assay (DIVA assay). We assayed the angio-inhibitory activity of the integrin-binding peptides identified in the original peptide array screening. Peptides 8, 8–9 and 9 were tested at 500 nM, as well

as peptides 9–13 and 9-13SCR at 1 μM local concentrations within the angioreactors, Figure 4c. Peptides 8 and 8–9 inhibited 70 ± 2% of the VEGF-A-induced angiogenic response and these values were statistically significant ($p<0.005$). Peptide 9 demonstrated the most potent activity with greater than 95% inhibition and was also highly significant with $p<0.0001$. Peptide 9–13 containing the C-terminal eight amino acids of peptide 9, showed significant ($p<0.05$) inhibition (~ 50% of the maximal response). However, when this sequence was scrambled (peptide 9-13SCR) the angio-inhibitory activity was completely depleted. Collectively these data strongly suggest that the α3β1 integrin-binding peptides identified in our TIMP-2 peptide array experiments have significant angio-inhibitory activity *in vivo*.

3.7 TIMP-2 integrin-binding peptide 8–9 demonstrates anti-tumorigenic activity *in vivo* in Kaposi's sarcoma model

The peptide 8–9 significantly reduced tumor growth when administered either by peritumoral injection (***$p< 0.01$, as determined by two-way ANOVA), Figure 5a, and intraperitoneal injection (data not shown). Differences became significant at day 7 after. The inhibitory effects were greater if animals received peptide by peritumoral injection. Microscopic examination of hematoxylin and eosin stained sections showed reduced cellularity and reduced vascularity of tumors in mice treated with peptide 8–9 (peritumoral and intraperitoneal), Figure 5c and 5d, as well as increased cellular necrosis, Figure 5d (intraperitoneal administration), that was not present in control mice treated with vehicle alone, Figure 5b. These data demonstrate that the TIMP-2 peptide 8–9 has statistically significant anti-tumor activity in this model of Kaposi's sarcoma.

4. Discussion

In addition to the studies by Seo et al. demonstrating the anti-mitogenic activity of TIMP-2 in hMVECs is α3β1-dependent, recent studies by Jaworski and colleagues demonstrate that TIMP-2 inhibits neurite outgrowth and promotes neurite differentiation *in vitro* via an α3β1 integrin-dependent mechanism [25]. These observations led the authors to suggest that up-regulation of TIMP-2 expression by proliferative stimuli results in the transition from neuronal proliferation to promotion of terminal neuronal differentiation. This concept is further supported by their subsequent demonstration that TIMP-2-deficient mice have a movement disorder with abnormal motor neuron development, and shows for the first time a significant phenotype for these TIMP-2 deficient mice [18]. These studies suggest that TIMP-2 binding to α3β1 and subsequent mediation of cell fate is not unique to hMVECs, and may be a more general biological mechanism of significance in control of tissue homeostasis.

Fernandez et al. [8] demonstrate that the C-terminal domain, specifically disulfide loop 6 of the TIMP-2 structure exhibits angio-inhibitory activity. It should be noted that the both the N-terminal TIMP-2 and mutant N-terminal TIMP-2, lacking MMP inhibitor activity, did show 35–40% inhibition of angiogenesis in their murine corneal pouch assay [8]. More recently Fernandez and colleagues have shown that a 24-mer loop 6 peptide binds to the ILGF-1R and that loop 6 binding to endothelial cells is completely independent of integrin α3β1 [9]. We did observe binding of ^{125}I-labeled C-terminal domain of TIMP-2 to hMVECs (Figure 1a) and this fragment did inhibit hMVEC proliferation in response to FGF-2 stimulation (data not shown), confirming the previous findings of Fernandez et al. [8]. However, our study focused on identifying the TIMP-2 region responsible for binding to the α3β1 integrin, and then evaluating the angio-inhibitory activity of protein fragments and synthetic peptides from this domain using hMVECs *in vitro* and the DIVA assay *in vivo*.

Our findings demonstrate that there is a 24 amino acid region located in the N-terminus of TIMP-2 that binds to integrin α3β1 and retains biological activity with respect to

suppression of VEGF-A-stimulated hMVEC growth *in vitro* as well as angio-inibition *in vivo*. Peptide binding arrays localized the α3β1 integrin-binding domain to a region containing the contiguous amino acid residues I^{43} through A^{66}, which includes portions of the B-β sheet, B-C loop and a few residues of the C-β-sheet structures, a region of the TIMP-2 structure previously characterized as highly flexible and solvent accessible [31]. The peptide array and synthetic peptide experiments suggest that further extension of the peptide sequence in the C-terminal direction from this peptide sequence results in a loss of integrin binding, growth inhibition and anti-angiogenic activity, confirming the distinct localization of integrin binding activity observed in the peptide array analysis. Our findings also suggest that small soluble peptides are capable of mimicking the integrin-binding and anti-angiogenic activity of the parent TIMP-2 protein, a principal well established for other extracellular matrix components such as IgG_1 [21], fibronectin [35], thrombospondin [3]. In fact many endogenous inhibitors of angiogenesis are indeed small peptide fragments of larger proteins and possess integrin-binding activity, e.g. angiostatin, endostatin, tumstatin, etc. [13, 23]. Furthermore, the findings in the present report confirm the previous observations that binding to α3β1 integrin is critical for the growth inhibitory and anti-angiogenic activity of TIMP-2 [17, 28, 29]. In addition, we demonstrate for the first time, that α3β1-binding peptides also show anti-tumorigenic activity in a murine Kaposi's sarcoma model. Sequence comparison of this region of TIMP-2 with that of the other mature human TIMPs was performed (using MacVector v 9.5.2). This analysis reveals several interesting features, Table 1. Overall the identities of the amino acid sequences compared to TIMP-2 are 44% for TIMP-1, 30% for TIMP-3 and 57% for TIMP-4. This contrasts with the comparison of the mature protein sequences in which identities relative to TIMP-2 are 53% for TIMP-1, 64% for TIMP-3, and 71% for TIMP-4. This suggests that the amino acid residue identity in this region of TIMP-2 is well below that observed for the overall sequence comparison. In addition, the TIMP-2 amino acid sequence in this region is unique in that it has a Pro residue at position 56 in the B-C loop followed by a series in which four out of the next five residues are charged amino acid residues. Both TIMP-1 and TIMP-4 contain Pro residues within the sequence regions corresponding to the TIMP-2 integrin-binding domain, these occur at the end of the sequences at the terminus of the C-β sheet structure [31]. TIMP-3 also contains a Pro residue at position 54 in B-C loop; it is not followed by charged amino acids as observed in the TIMP-2 B-C loop. These findings are consistent with previous observations suggesting that the largest differences in amino acid sequence between the TIMP families are found in these exposed loop regions including the A-B loop, the loop before entering the D strand, as well as the B-C loop where it enters the C-strand. This B-C loop was identified in the present study as the putative α3β1-binding region [31]. NMR and x-ray diffraction studies of TIMP-1 and TIMP-2 in complex with the active site of a MMP, as well as in solution have shown that the overall structure is that of an oligonucleotide/oligosaccharide-binding (OB) fold in which the N-terminal domain is dominated by a β-barrel structure [10, 12, 31, 32]. Examination of the structure of the TIMP-2 shows that the B-C loop and the short extension into the C strand that comprise the putative integrin-binding region are located on the surface of the molecule and are solvent accessible (Figure 6a and 6b). Furthermore, comparison with the structure of TIMP-2 and TIMP-1 in this region, the only other member of the TIMP family for which structure information is available in the Research Collaboratory for Structural Bioinformatics Protein Data Base, reveals some interesting differences. The integrin peptide binding sequence centers on the B-C loop region, which is between the B and C β-sheet strands of the parent molecules. Alignment of the B-C loop regions of TIMP-1 and TIMP-2 shows that the Pro residue at position 56 (P^{56}) induces a severe bend in the peptide backbone resulting in a significant departure from the TIMP-1 structure (Figure 6 b & c, Table 1). Immediately C-terminal to this bend one observes that the side chains of the Glu residue at position 57 (E^{57}), Lys residue at position 58 (K^{58}), the Asp residue at position 59 (D^{59}), as well as the Glu residue at position 61 (E^{61}) all project away from the internal region of the β barrel and

are directed towards the hydration sphere/solvent interface. This is apparent when observed with the B-C loop aligned perpendicular to the long axis of the OB-fold (Figure 6c) or if the B-C loop is observed from above (Figure 6d). These residues form a charged polar surface and form a potential integrin-binding site. This is an interesting observation in light of the fact that classic integrin-binding sequences, e.g. RGD, often contain charged residues and it has recently been demonstrated that Glu residues are critical determinants of laminin α chain binding to integrins [16]. Also, as previously demonstrated, TIMP-2 binding to α3β1 integrin is divalent cation-dependent [28].

The N-terminal domains of the TIMPs also share sequence homology and structural similarities with netrins, complement proteins (C3, C4 and C5), secreted frizzled-related proteins and type I procollagen C-proteinase enhancer [1], and this region is known as the netrin (NTR) module. These proteins perform diverse biological roles including the control of astacin-like metalloproteinase activity of bone morphogenic protein 1 (BMP1), regulation of Wnt signaling, as well as regulation of axon guidance and angiogenesis. Interestingly members of the netrin family, including netrin 1, function as axonal and endothelial guidance cues. In addition to the classic netrin receptors, such as UNC5 and deleted in colon carcinoma (DCC), the effects of netrins may also be mediated by signaling pathways initiated via binding to α3β1 and α6β4 integrins [4, 22]. However, two important differences between TIMP-2 and netrin 1 are: 1) whereas TIMP-2 is anti-angiogenic, netrins are pro-angiogenic [24, 33]; 2) the α3β1-binding site of TIMP-2 is in the B-C loop which is approximately in the middle of the NTR module, the integrin binding domain of the netrins is localized very close to the C-terminus of this molecule and is quite distinct in sequence from the TIMP-2 B-C loop [36]. The differences in the binding domains may account for the converse effects of these two molecules on angiogenesis.

In summary, we have identified a peptide region of TIMP-2 that centers on the B-C loop region of the TIMP-2 molecule that retains α3β1 integrin-binding activity, as well as endothelial growth suppression, anti-angiogenic activity and anti-tumorigenic activity *in vivo*. Examination of this region demonstrates that the amino acid sequence in this region is rather unique compared with other members of the TIMP family and that it has an unusual structure that may form a potential integrin-binding site. As suggested by Fernandez and colleagues, it is possible that intact TIMP-2 may interact with both the IGF-1R and α3β1 at the same time [9]. Although interaction with either receptor may be sufficient to inhibit endothelial mitogenic responses *in vitro* and angiogenesis, it is also possible simultaneous binding to both receptors may enhance inhibition of angiogenesis. Such experiments can now be conducted with the identification of loop 6 and current identification of α3β1-binding peptides. In conclusion, our work supports the concept that TIMP-2 has potent anti-angiogenic activity that is mediated by three distinct mechanisms: inhibition of critical MMPs, such as MT1-MMP; and direct inhibition endothelial cell growth, mediated by binding to IGF-1R and/or integrin α3β1.

Highlights

An Integrin-binding N-terminal Peptide Region of TIMP-2 Retains Potent Angio-Inhibitory and Anti-tumorigenic activity *In Vivo*

Seo et al.,

The α3β1 binding domain is localized to the N-terminal domain of the TIMP-2.

This integrin binding domain encompases residues Ile43-Ala66, or B-C loop.

Synthetic peptides containing sequences from this region suppress endothelial growth.

Peptides from this region are anti-angiogenic and anti-tumorigenic *in vivo*.

These data suggest that TIMP-2 binds to the endothelial cell surface through two distinct mechanisms: loop 6, as demonstrated by Fernandez and colleagues, and B-C loop as demonstrated here.

Supplementary Material

Refer to Web version on PubMed Central for supplementary material.

Acknowledgments

This work was supported by intramural research funds from the National Cancer Institute, Center for Cancer Research Project # Z01SC009179.

References

1. Banyai L, Patthy L. The NTR module: domains of netrins, secreted frizzled related proteins, and type I procollagen C-proteinase enhancer protein are homologous with tissue inhibitors of metalloproteases. Protein Science. 1999; 8:1636–1642. [PubMed: 10452607]
2. Brew K, Dinakarpandian D, Nagase H. Tissue inhibitors of metalloproteinases: evolution, structure and function. Biochim Biophys Acta. 2000; 1477:267–283. [PubMed: 10708863]
3. Calzada MJ, Roberts DD. Novel integrin antagonists derived from thrombospondins. Current Pharmaceutical Design. 2005; 11:849–866. [PubMed: 15777239]
4. Cirulli V, Yebra M. Netrins: beyond the brain. Nature Reviews Molecular Cell Biology. 2007; 8:296–306.
5. D'Alessio S, Ferrari G, Cinnante K, Scheerer W, Galloway AC, Roses DF, et al. Tissue Inhibitor of Metalloproteinases-2 Binding to Membrane-type 1 Matrix Metalloproteinase Induces MAPK Activation and Cell Growth by a Non-proteolytic Mechanism. J Biol Chem. 2008; 283:87–99. [PubMed: 17991754]
6. DeClerck YA, Yean TD, Lee Y, Tomich JM, Langley KE. Characterization of the functional domain of tissue inhibitor of metalloproteinases-2 (TIMP-2). Biochem J. 1993; 289(Pt 1):65–69. [PubMed: 8424773]
7. Emmert-Buck MR, Emonard HP, Corcoran ML, Krutzsch HC, Foidart JM, Stetler-Stevenson WG. Cell surface binding of TIMP-2 and pro-MMP-2/TIMP-2 complex. FEBS Letters. 1995; 364:28–32. [PubMed: 7750537]
8. Fernandez CA, Butterfield C, Jackson G, Moses MA. Structural and functional uncoupling of the enzymatic and angiogenic inhibitory activities of tissue inhibitor of metalloproteinase-2 (TIMP-2): loop 6 is a novel angiogenesis inhibitor. Journal of Biological Chemistry. 2003; 278:40989–40995. [PubMed: 12900406]
9. Fernandez CA, Roy R, Lee S, Yang J, Panigrahy D, Van Vliet KJ, et al. The anti-angiogenic peptide, loop 6, binds insulin-like growth factor-1 receptor. J Biol Chem. 2010; 285:41886–41895. [PubMed: 20940305]
10. Fernandez-Catalan C, Bode W, Huber R, Turk D, Calvete JJ, Lichte A, et al. Crystal structure of the complex formed by the membrane type 1-matrix metalloproteinase with the tissue inhibitor of metalloproteinases-2, the soluble progelatinase A receptor. EMBO Journal. 1998; 17:5238–5248. [PubMed: 9724659]
11. Ferrari N, Morini M, Pfeffer U, Minghelli S, Noonan DM, Albini A. Inhibition of Kaposi's sarcoma in vivo by fenretinide. Clinical Cancer Research. 2003; 9:6020–6029. [PubMed: 14676128]
12. Gomis-Ruth FX, Maskos K, Betz M, Bergner A, Huber R, Suzuki K, et al. Mechanism of inhibition of the human matrix metalloproteinase stromelysin-1 by TIMP-1. Nature. 1997; 389:77–81. [PubMed: 9288970]
13. Grant MA, Kalluri R. Structural basis for the functions of endogenous angiogenesis inhibitors. Cold Spring Harb Symp Quant Biol. 2005; 70:399–410. [PubMed: 16869777]

14. Guedez L, Rivera AM, Salloum R, Miller ML, Diegmueller JJ, Bungay PM, et al. Quantitative assessment of angiogenic responses by the directed in vivo angiogenesis assay. Am J Pathol. 2003; 162:1431–1439. [PubMed: 12707026]
15. Hoegy SE, Oh HR, Corcoran ML, Stetler-Stevenson WG. Tissue inhibitor of metalloproteinases-2 (TIMP-2) suppresses TKR-growth factor signaling independent of metalloproteinase inhibition. Journal of Biological Chemistry. 2001; 276:3203–3214. [PubMed: 11042184]
16. Ido H, Ito S, Taniguchi Y, Hayashi M, Sato-Nishiuchi R, Sanzen N, et al. Laminin isoforms containing the gamma3 chain are unable to bind to integrins due to the absence of the glutamic acid residue conserved in the C-terminal regions of the gamma1 and gamma2 chains. Journal of Biological Chemistry. 2008; 283:28149–28157. [PubMed: 18697739]
17. Jaworski DM, Perez-Martinez L. Tissue inhibitor of metalloproteinase-2 (TIMP-2) expression is regulated by multiple neural differentiation signals. Journal of Neurochemistry. 2006; 98:234–247. [PubMed: 16805810]
18. Jaworski DM, Soloway P, Caterina J, Falls WA. Tissue inhibitor of metalloproteinase-2(TIMP-2)-deficient mice display motor deficits. Journal of Neurobiology. 2006; 66:82–94. [PubMed: 16216006]
19. Kim PJ, Sakaguchi K, Sakamoto H, Saxinger C, Day R, McPhie P, et al. Colocalization of heparin and receptor binding sites on keratinocyte growth factor. Biochemistry. 1998; 37:8853–8862. [PubMed: 9636026]
20. Lambert E, Dasse E, Haye B, Petitfrere E. TIMPs as multifacial proteins. Critical Reviews in Oncology Hematology. 2004; 49:187–198.
21. Morgan EL, Hugli TE, Weigle WO. Isolation and Identification of a Biologically Active Peptide Derived from the CH3 Domain of Human IgG1. Proceedings of the National Academy of Sciences. 1982; 79:5388–5391.
22. Nikolopoulos SN, Giancotti FG. Netrin-integrin signaling in epithelial morphogenesis, axon guidance and vascular patterning. Cell Cycle. 2005; 4:e131–e135. [PubMed: 15725728]
23. Nyberg P, Xie L, Kalluri R. Endogenous inhibitors of angiogenesis. Cancer Res. 2005; 65:3967–3979. [PubMed: 15899784]
24. Park KW, Crouse D, Lee M, Karnik SK, Sorensen LK, Murphy KJ, et al. The axonal attractant Netrin-1 is an angiogenic factor. Proceedings of the National Academy of Sciences of the United States of America. 2004; 101:16210–16215. [PubMed: 15520390]
25. Perez-Martinez L, Jaworski DM. Tissue inhibitor of metalloproteinase-2 promotes neuronal differentiation by acting as an anti-mitogenic signal. J Neurosci. 2005; 25:4917–4929. [PubMed: 15901773]
26. Saxinger, C. Automated Peptide Design and Synthesis. In: Office USP. , editor. United States: National Institutes of Health; 2000.
27. Saxinger C, Conrads TP, Goldstein DJ, Veenstra TD. Fully automated synthesis of (phospho)peptide arrays in microtiter plate wells provides efficient access to protein tyrosine kinase characterization. BMC Immunology. 2005; 6:1. [PubMed: 15647109]
28. Seo DW, Li H, Guedez L, Wingfield PT, Diaz T, Salloum R, et al. TIMP-2 mediated inhibition of angiogenesis: an MMP-independent mechanism. Cell. 2003; 114:171–180. [PubMed: 12887919]
29. Seo DW, Li H, Qu CK, Kim YS, Diaz T, Wei B, et al. Shp-1 mediates the antiproliferative activity of tissue inhibitor of metalloproteinase-2 in human microvascular endothelial cells. Journal of Biological Chemistry. 2006; 281:3711–3721. [PubMed: 16326706]
30. Stetler-Stevenson WG. The tumor microenvironment: regulation by MMP-independent effects of tissue inhibitor of metalloproteinases-2. Cancer Metastasis Rev. 2008; 27:57–66. [PubMed: 18058195]
31. Tuuttila A, Morgunova E, Bergmann U, Lindqvist Y, Maskos K, Fernandez-Catalan C, et al. Three-dimensional structure of human tissue inhibitor of metalloproteinases-2 at 2.1 A resolution. Journal of Molecular Biology. 1998; 284:1133–1140. [PubMed: 9837731]
32. Williamson RA, Martorell G, Carr MD, Murphy G, Docherty AJ, Freedman RB, et al. Solution structure of the active domain of tissue inhibitor of metalloproteinases-2. A new member of the OB fold protein family. Biochemistry. 1994; 33:11745–11759. [PubMed: 7918391]

33. Wilson BD, Ii M, Park KW, Suli A, Sorensen LK, Larrieu-Lahargue F, et al. Netrins promote developmental and therapeutic angiogenesis. Science. 2006; 313:640–644. [PubMed: 16809490]

34. Wingfield PT, Sax JK, Stahl SJ, Kaufman J, Palmer I, Chung V, et al. Biophysical and functional characterization of full-length, recombinant human tissue inhibitor of metalloproteinases-2 (TIMP-2) produced in Escherichia coli. Comparison of wild type and amino-terminal alanine appended variant with implications for the mechanism of TIMP functions. Journal of Biological Chemistry. 1999; 274:21362–21368. [PubMed: 10409697]

35. Yamada KM, Kennedy DW. Dualistic Nature of Adhesive Protein Function: Fibronectin and Its Biologically Active Petide Fragments Can Autoinhibit Fibronectin Fuction. J Cell Biol. 1984; 99:29–36. [PubMed: 6736130]

36. Yebra M, Montgomery AM, Diaferia GR, Kaido T, Silletti S, Perez B, et al. Recognition of the neural chemoattractant Netrin-1 by integrins alpha6beta4 and alpha3beta1 regulates epithelial cell adhesion and migration. Developmental Cell. 2003; 5:695–707. [PubMed: 14602071]

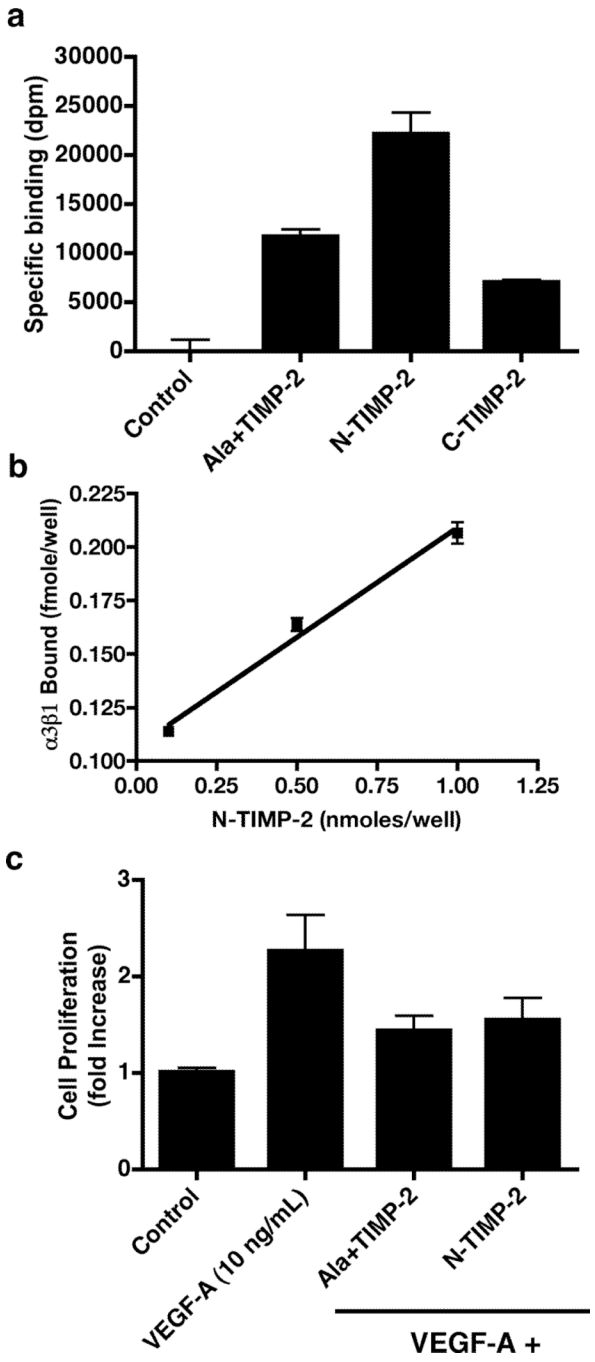

Figure 1.

The N-terminal domain of TIMP-2 demonstrates enhanced α3β1 integrin-binding activity and retains anti-mitogenic activity. a) Integrin α3β1-binding to Ala+TIMP-2, N-TIMP-2 and C-TIMP-2/GST-fusion proteins. Wells of Maxisorb™ 96 well plates were coated with protein solutions, blocked and probed for integrin binding activity as described in Materials and Methods. Integrin-binding to N-TIMP-2 was two fold greater compared with Ala +TIMP-2 and three fold greater than C-TIMP-2 (* $p<0.0001$). The results demonstrate that the N-terminal region of the TIMP-2, containing the OB fold has the most potent α3β1-binding activity. α3β1-binding to N-TIMP-2 was 2.5 fold increased over binding to Ala +TIMP-2 when values are normalized for coating concentrations. b) Binding of α3β1 to N-

TIMP-2 shows concentration dependence and is linear (R^2= 0.9881) over the range of protein coating concentrations tested. Assuming saturation binding for the coating protein on the Maxisorb™ plates, the calculated dissociation constants (K_D) for the α3β1-binding interaction with N-TIMP-2 were 0.35, 0.12 and 0.19 nM for the 1, 5 and 10 μM coating concentrations, respectively, and the mean value was K_D ~0.22 ± 0.12 nM. These values are in excellent agreement with values previously reported for TIMP-2 binding to the cell surface in an α3β1-dependent fashion (K_D=0.9 ± 0.12 nM) and are consistent with the approximate 2.5 fold increase in N-TIMP-2 binding compared with Ala+TIMP-2 binding observed in Figure 1a. c) The N-terminal α3β1-binding domain of TIMP-2 retains anti-mitogenic activity. VEGF-A-stimulated (10 ng/mL) hMVECs demonstrate greater than two-fold increase in cell number after 24 h compared with control (untreated cells). Ala+TIMP-2 and N-TIMP-2 significantly inhibited the mitogenic response to VEGF-A in vitro, * $p<0.0001$.

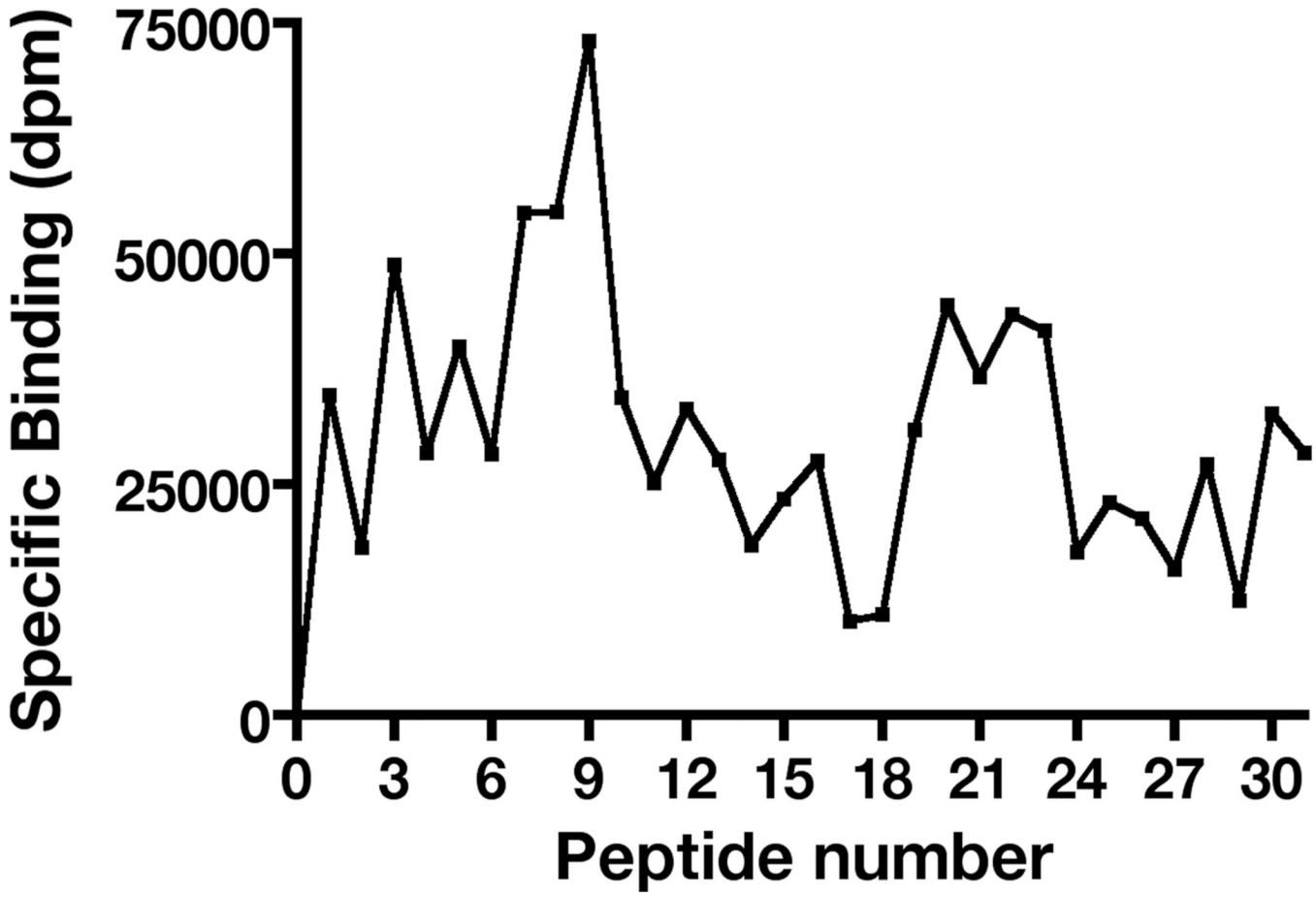

Figure 2.

Peptide array analysis of α3β1-binding to TIMP-2 defines a unique integrin-binding domain. α3β1-binding to TIMP-2 18-mer peptides mapped across the entire TIMP-2 sequence. The results demonstrated a clear peak of binding activity in the well containing peptide 9, with significant binding in the immediate N-terminal adjacent peptide sequences (peptides 8 and 7, see text). However, the α3β1-binding to peptides immediately C-terminal to peptide 9 was significantly diminished.

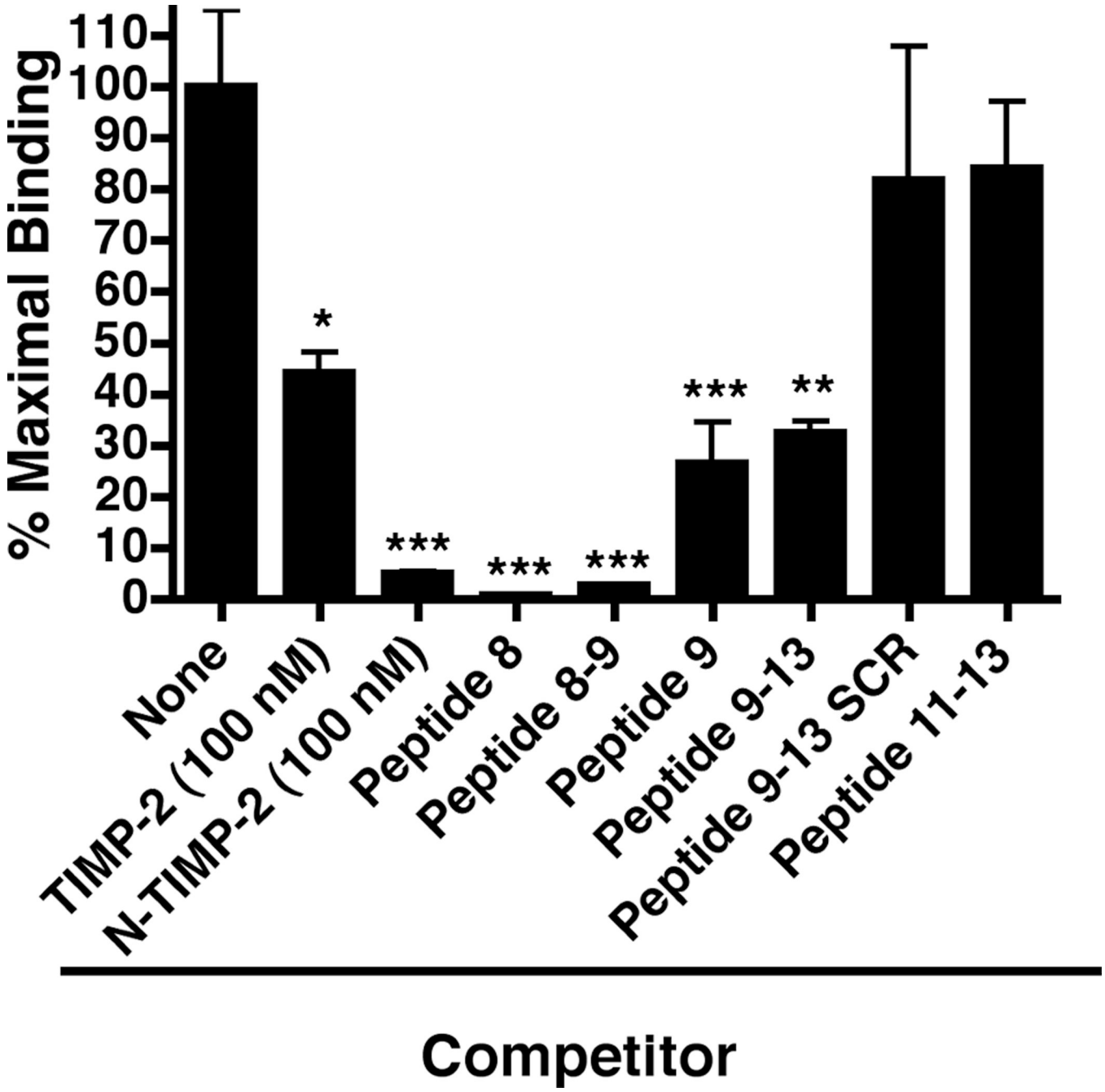

Figure 3.

Peptide competition experiments for α3β1-binding. Wells were coated with Ala+TIMP-2 and blocked as descried in Materials and methods. The α3β1-binding activity was then assayed in the absence (maximal binding) or the presence of TIMP-2 (100 nM, * $p<0.01$), N-TIMP-2 (100 nM, *** $p<0.0005$), or synthetic peptides (all added at 1 μM final concentration). The results demonstrate that peptide 8, peptide 9, as well as the overlap region between these two peptides, peptide 8–9 significantly (*** $p<0.0005$) compete for the ability of α3β1-binding to the Ala+TIMP-2 coating (see Supplemental Data Table 2 for specific peptide sequences). In addition, the results confirm the importance of the C-terminal portion of peptide 9 in α3β1-binding, in that peptide 9–13 retains significant (** $p<0.005$)

competitive activity, whereas loss of peptide 9 sequence as in peptide 11–13 or disruption of the linear peptide 9 sequence (peptide 9–13 SCR) resulted in substantial loss of competitive binding activity. The results confirm the findings of the peptide array analysis of TIMP-2 peptides.

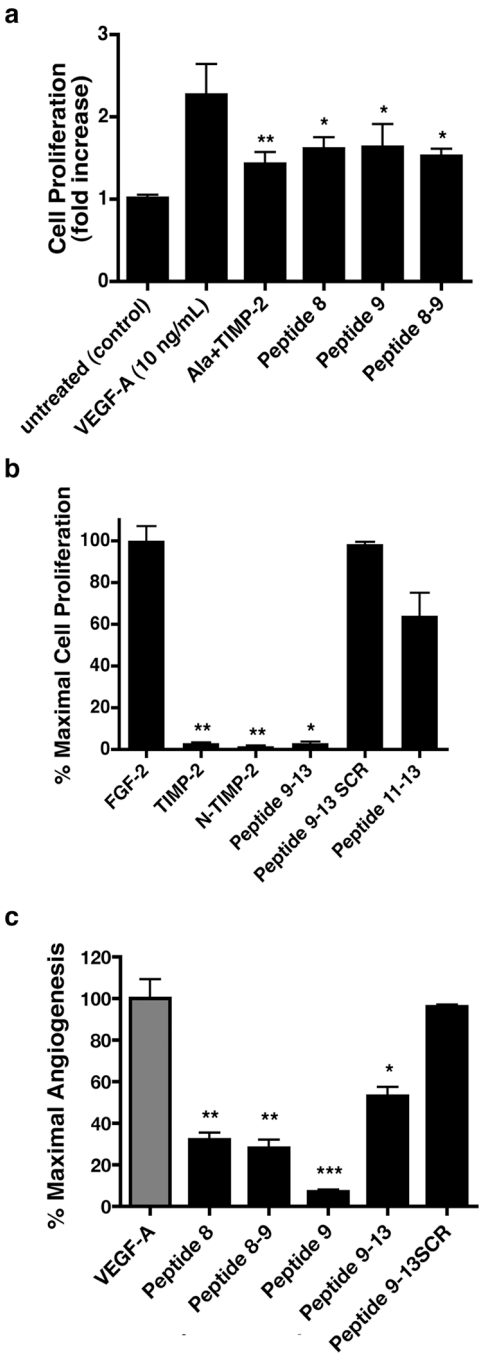

Figure 4.

TIMP-2 α3β1-binding peptides retain anti-mitogenic activity in vitro and anti-angiogenic activity *in vivo*. a) VEGF-A-stimulated (10 ng/mL) hMVECs demonstrate greater than two-fold increase in cell number after 24 h. TIMP-2 α3β1-binding peptides, peptide 8, peptide 9 and peptide 8–9 at 1 μM concentrations are essentially equipotent with 100 nM Ala+TIMP at inhibition of the VEGF-A-induced mitogenic response in hMVEC *in vitro*. Statistical analysis: ** denotes $p<0.001$ and * denotes $p\leq0.01$. b) FGF-2-stimulated mitogenic response of hMVECs was also inhibited by TIMP-2 as previously reported. In addition, mitogenic stimulation of hMVECs was also inhibited by N-TIMP-2, and by the peptide containing the eight C-terminal amino acid residues of peptide 9, peptide 9–13, but loss of

this peptide 9 sequence (peptide 11–13) or disruption of the primary sequence of peptide 9 (peptide 9–13 SCR) sequence resulted in significant loss of anti-mitogenic activity. Statistical analysis: ** denotes $p<0.0005$; * denotes $p<0.005$. c) The α3β1-binding TIMP-2 peptides retain anti-angiogenic activity in vivo. The α3β1-binding peptides, peptide 8, peptide 8–9, peptide 9, as well as peptide 9–13 and 9–13SCR were tested for anti-angiogenic activity using the directed in vivo angiogenesis assay [14, 28, 29]. The results demonstrate that at 0.5 μM local concentration of peptides 8, 8–9 and 9 showed statistically significant inhibition of angiogenic activity in vivo. The angio-inhibitory activity of peptide 9–13 was somewhat less (~ 50 %) but remained statistically significant. However, scrambling peptide 9–13 sequence destroyed this angio-inhibitory activity. Statistical analysis: *** denotes $p<0.0001$, ** denotes $p<0.0005$ and * denotes $p<0.05$.

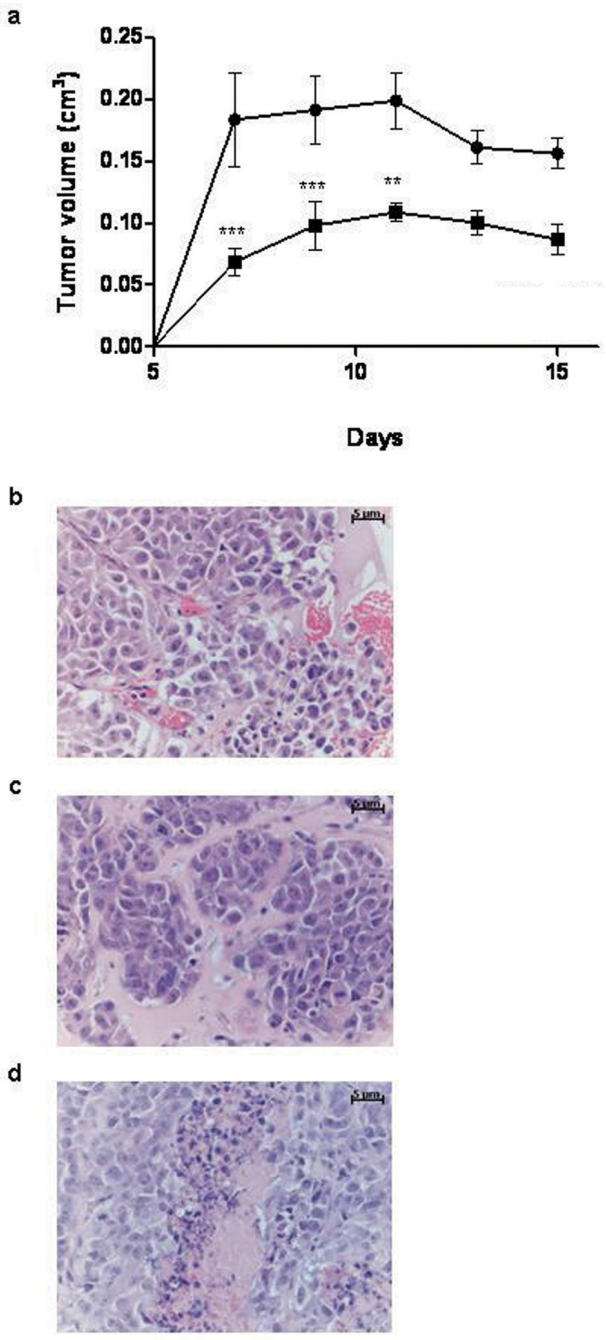

Figure 5.

Peptide 8–9 demonstrates anti-tumorigenic activity in a murine Kaposi's sarcoma model. Seven-week-old nude mice were injected in the flank with 5×10^6 KS-IMM cells. Animals received peritumoral injection (or intraperitoneal injection, data not shown) of 150 μL of 500 nM peptide 8–9 three times a week starting on day 0 (-■-). Control animals were injected with vehicle alone (-●-). a) Tumor growth was significantly reduced by peritumoral with peptide 8–9 treatment compared to vehicle alone (***$p < 0.001$, **$p < 0.01$, two-way ANOVA). b) Histology of treated and untreated tumors. Peritumoral (c) and intraperitoneal (d) treatments with peptide 8–9 resulted in a decrease in tumor vascularity and cellularity compared with control tumor (b) (magnification 400×).

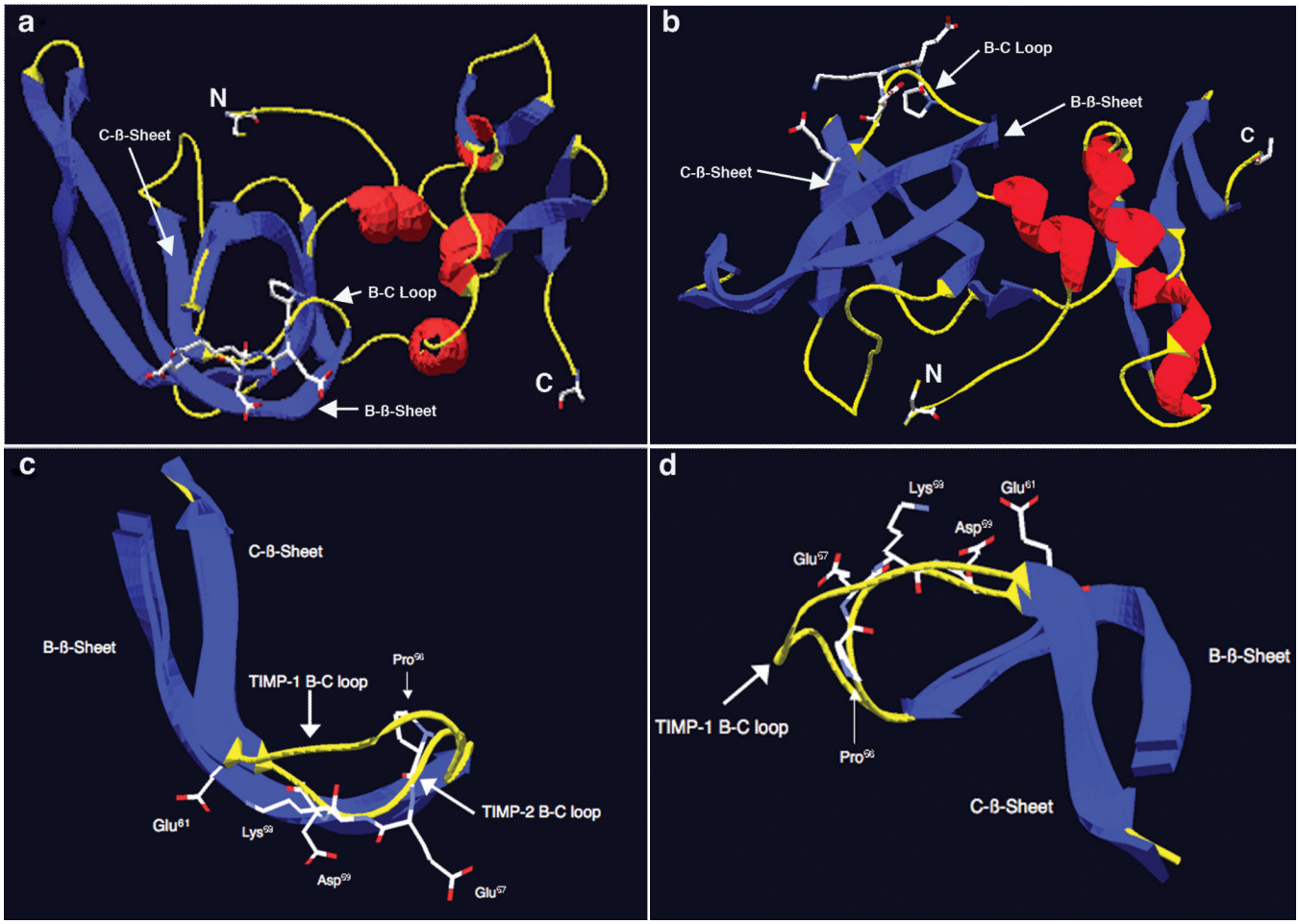

Figure 6.

Structure analysis and identification of potentially important amino acid residues for the α3β1-binding activity of TIMP-2 localized to the B-C loop. a) Structure of TIMP-2 viewed perpendicular to the long axis of the N-terminal OB fold. Blue denotes β-sheets, red denotes α-helices and yellow denotes loop structures. N is the amino terminal cysteine and C is the carboxyl terminal alanine residue. Also shown is the surface localization of the charged residues of the 23 amino acid α3β1-binding region of the B-C loop. b) Structure of TIMP-2 viewed from below, all other designations are the same as in A. c) B-C loops of TIMP-2 and TIMP-1 overlaid and viewed perpendicular to the long axis of the OB fold, demonstrating the kink induced by Pro^{56} that results in projection of the charged amino acid residues Glu^{57}, Lys^{58}, Asp^{59} and Glu^{61} of the 24 amino acid α3β1-binding domain away from the interior of the OB fold towards the surface of the TIMP-2 molecule. d) B-C loops of TIMP-2 and TIMP-1 viewed from above again showing projection of amino acid residues Glu^{57}, Lys^{58}, Asp^{59} and Glu^{61} towards the surface and away from the interior of the TIMP-2 molecule.

Table 1

Comparison of human TIMP aligned sequences in α3β1 integrin-binding region.

Asterisks (*) denote sequence identity. Double arrows indicate sequences of TIMP-2 peptides 8 and 9.